EFFICIENCY OF BUTTRESS WALLS IN DEEP EXCAVATIONS

Shong-Loong Chen [1], Cheng-Tao Ho [2], Chong-Dao Li [3], and Meen-Wah Gui [4]

ABSTRACT

Buttress walls have been widely adopted, with many successful cases, in soft ground excavation work. The field instrumented displacement data indicated that buttress walls could effectively reduce the lateral displacement of diaphragm wall and thus enhance the stability of the excavation work. The interaction between the soil/buttress- and diaphragm walls is a three dimensional problem but in practice, due to the complexity of three-dimensional analysis, the problem is commonly simplified into a two-dimensional problem. The simplification becomes irrational if the excavation site is almost square. This study aimed at examining the influence of the geometry of the buttress walls (shape, thickness, and length) on the displacement of buttressed diaphragm wall via a series of three-dimensional analysis. The relative effectiveness of the internal and external buttress walls and of the chipping-off and non chipping-off buttress walls on the displacement of the diaphragm wall were also studied. The numerical procedure was first calibrated against the field data obtained from the Taipei 101 and Neihu basements excavation projects. These results were evaluated and compared through the so-called displacement reduction ratio (DRR). The results indicated that the effective spacing of the buttress walls should be within two times the excavation depth and that the *T*-shaped buttress wall was more efficient than the *I*-shaped buttress walls. In addition, to achieve optimum performance in minimizing diaphragm wall displacement, the buttress walls should not be sequentially removed during the excavation stages.

Key words: Soft ground excavation, buttressed diaphragm wall, wall displacement, three-dimensional FE analysis.

1. INTRODUCTION

To maintain the integrity of adjacent buildings and, at the same time, enhance the stability of deep supported excavation in soft-ground, it is often necessary to limit the lateral displacement of the support structure such as diaphragm wall. There are many options for geotechnical design engineer to choose from in order to reduce the displacement of the diaphragm wall used in deep excavation; for examples, ones may choose to increase the thickness of the diaphragm wall or strengthen the bracing of the diaphragm wall, use buttress walls, cross walls, ground improvement technique, *etc*. Of these options, successful applications of buttress walls have been observed in many of the excavation projects in Taiwan. However, in practice, the analysis of the buttressed diaphragm wall is usually simulated by simplifying the problem into a two-dimensional problem. For example, to analyze the behavior of buttressed diaphragm wall, Hsieh and Lu (1999) developed a simplified method to represent the three-dimensional behavior of buttressed diaphragm walls. The simplified method was adopted in the "beam-on-elasto-plastic-foundation" programs such as RIDO and TORSA (Taiwan Originated Retaining Structure Analysis). This method has since become the common method for buttress walls analysis in Taiwan. However, the simplified analysis failed to capture the true interaction between the excavation and the buttressed diaphragm wall, which is essentially a three-dimensional (3D) behavior.

Of course, ones could deduce the maximum wall movement induced by deep excavation using semi-empirical method, which had been calibrated against 3D finite element analyses. For examples, Ou *et al*. (1996) proposed a relationship to estimate the three-dimensional maximum wall displacement of an excavation based on a series of two-dimensional finite element analysis, and using the concept of PSR (plane strain ratio) proposed by Ou *et al*. (1996), Finno *et al*. (2007) related the maximum movement in the center of an excavation wall computed by three-dimensional analyses to that obtained by plane strain analyses.

Nevertheless, Ou *et al*. (1996), who evaluated the corner effects of an irregular-shaped excavation project in Taipei, concluded that deformation behavior of a short primary wall can be heavily affected by the corners. Finno *et al*. (2007), who studied the effects of excavation geometry (length, width, and depth of excavation), wall stiffness, and factor of safety against basal heave on the three-dimensional ground movements caused by excavation in clays, also pointed out the significance of corner effects on the deformation of diaphragm wall. From their three-dimensional finite element analysis on a real excavation project, Ou *et al*. (2008) concluded that the buttressed diaphragm wall displacements were influenced by the penetration depth of the *T*-shaped buttress walls in the hard soil layer where the diaphragm wall deformation would be effectively reduced if the buttress walls ended in the hard soil. However, the degree of the influence of the spacing between the buttress walls, and the relative effectiveness of the *I*-shaped buttress wall against the *T*-shaped buttress wall are still not well understood.

Manuscript received May 18, 2011; revised December 2, 2011; accepted December 6, 2011.

[1] Associate Professor, Dept. of Civil Eng., National Taipei University of Technology, Taipei 10608, Taiwan, R.O.C. (e-mail: f10391@ntut.edu.tw).

[2] Ph.D. candidate, Graduate Institute of Engineering Technology, National Taipei University of Technology, Taipei 10608, Taiwan, R.O.C. (e-mail: s4679005@ntut.org. tw).

[3] Former graduate student, Graduate Institute of Civil and Disaster Prevention Engineering, National Taipei University of Technology, Taipei 10608, Taiwan, R.O.C. (e-mail: davidpip@msn.com).

[4] Associate Professor (corresponding author), Dept. of Civil Eng., National Taipei University of Technology, Taipei 10608, Taiwan, R.O.C. (e-mail: mwgui@ntut.edu.tw).

Using the three-dimensional numerical program "Plaxis 3D-Foundation" (Brinkgreve and Swolfs 2007), this study aims at examining the influence of the geometry of the buttress walls (shape, thickness, and length) on the displacement of buttressed diaphragm wall. The relative effectiveness of the internal and external buttress walls and of the chipping-off and non chipping-off buttress walls on the displacement of the diaphragm wall are also studied. The numerical procedure is first calibrated against the field data obtained from the Taipei 101 and Neihu basements excavation projects. Subsequently, the relatively less complicated Neihu project is selected as the model for the parametric study of the geometrical effects of the buttress walls. These results are evaluated and compared through the so-called displacement reduction ratio (DRR), which is essentially the relative amount of displacement generated by the diaphragm walls with and without buttress walls.

2. TAIPEI 101 PROJECT AND NUMERICAL ANALYSIS

2.1 Project Background

Taipei 101, a 101-storey skyscraper, is the world second tallest building that is situated in the Xinyi District of Taipei City. The construction site consisted of an *L*-shape podium zone and a rectangular tower zone, both with an integrated 5-storey basement excavated to a depth of about 22 m. The podium has a 6-storey shopping mall (five above and one underground) and 4-level of underground car parks while the tower has 101 floors and 5-level of underground car parks. The 152 m wide by 155 m long basement was bounded by diaphragm walls (Fig. 1(a)); the rectangular tower zone occupied an area of 87 m × 95 m in plan while the *L*-shape podium occupied the rest of the area bounded by the diaphragm walls. The tower was constructed up to the 91st floor at the height of 391 m, the tower-top was built to the 101st floor at the height of 438 m, the roof was constructed to the height of 448 m, and finally a 60 m pinnacle was erected to the spire at the height of 508 m (Yu 2011). Two different construction methods have been used in this project. The top-down construction method with concrete floor slabs as bracing system was used for the podium basement while the bottom-up construction method with pre-loaded steel strut, Fig. 1(b), was used for the tower basement. Diaphragm walls with a thickness of 1.2 m were used as the underground retaining structure and the internal walls separating the podium and the tower basements. The diaphragm-wall was socketed 1 m into the rock formation and thus the depths of the wall varied between 40 to 55 m. This study specifically models the response of the excavation of the tower zone only [Figs. 1(b) and 1(c)]. To reduce the wall deformation, these diaphragm walls have been strengthened by internal and external buttress walls, as shown in Fig. 1(c). All the buttress walls were 6 m in length and their thickness and depth were identical to that of the buttressed diaphragm walls, Fig. 1(d). The excavation of the tower basement was divided into seven construction stages with six levels of pre-loaded steel struts (bracing system) (see Fig. 2). The first level of the bracing system was strutted by four numbers of H350 × 350 × 12 × 19 structural steel members while the bracing system for levels two to six was four number of H400 × 400 × 13 × 21 structural steel members. Intermediate columns were H400 × 400 × 13 × 21 structural steel members.

2.2 Input Parameters

As reported by Lin and Woo (2005, 2007), a total of 128 boreholes had been drilled for the study site, which was located at the southeast boundary of the Taipei basin. A series of laboratory testing and field tests have been conducted to determine the physical and mechanical properties of the study ground (Lin and Woo 2007). The laboratory tests included triaxial UU, CIU, CK_oU-AC tests, uniaxial compression test and permeability test. The field tests encompassed standard penetration test, vane shear test, geophysical exploration and in-situ permeability test. These tests results have been summarized and presented by Lin and Woo (2005, 2007) for used in their geotechnical analyses of pile-raft foundation and deep excavation. For ease of reference, their effective stress soil parameters and soil models used are represented here in Table 1. The ground water table was located at approximately 0.5 m below the ground surface of the study site.

Note that Plaxis uses a different approach in modeling the undrained behavior of soil; it allows users to model the undrained behavior in an effective stress analysis using the effective stress parameters by simply assigning the material behavior of a soil layer as undrained (Brinkgreve and Swolfs 2007). In this case, PLAXIS automatically uses a bulk stiffness for the water and distinguishes between total stresses, effective stresses and excess pore pressures In addition, for undrained material behavior the effective Poisson's ratio should be smaller than 0.35 because using higher values of Poisson's ratio would mean that the water would not be sufficiently stiff with respect to the soil skeleton (Brinkgreve and Swolfs 2007). The material behavior of the CL soil layers were switched to undrained in this study.

The parameters for the diaphragm wall, floor slab, buttress walls and steel struts are given in Table 2. The Young's modulus of the concrete diaphragm wall, concrete floor slabs and concrete buttress wall were determined from their respective compressive strength, f_c' , using the equation $E_c = 4700\sqrt{f_c'}$ MPa, where f_c' is in MPa. However, a reduction factor of 0.6 should be applied to these Young's modulus values, including the one for the steel struts, to cater for the concrete cracking due to wall deformation, lack of fit and the possibility of poor construction quality. Ou *et al*. (1998) found that the value of the above reduction factor was reasonable.

2.3 Numerical Modeling

The geometry of the tower excavation site was 87 m × 95 m in plan, which was basically a square site. Therefore, it was unacceptable to simplify the excavation analysis into a plane strain analysis if true response of the diaphragm wall was to be obtained. A three-dimensional analysis was thus required. The three-dimensional numerical model for the whole construction site is shown in Fig. 3. The width of the model boundary was taken to be 5 times the excavation depth from each side of the diaphragm wall and the boundaries of the model were assumed to be fixed. The excavation procedure for the tower basement adopted in the numerical analysis is outlined in Table 3.

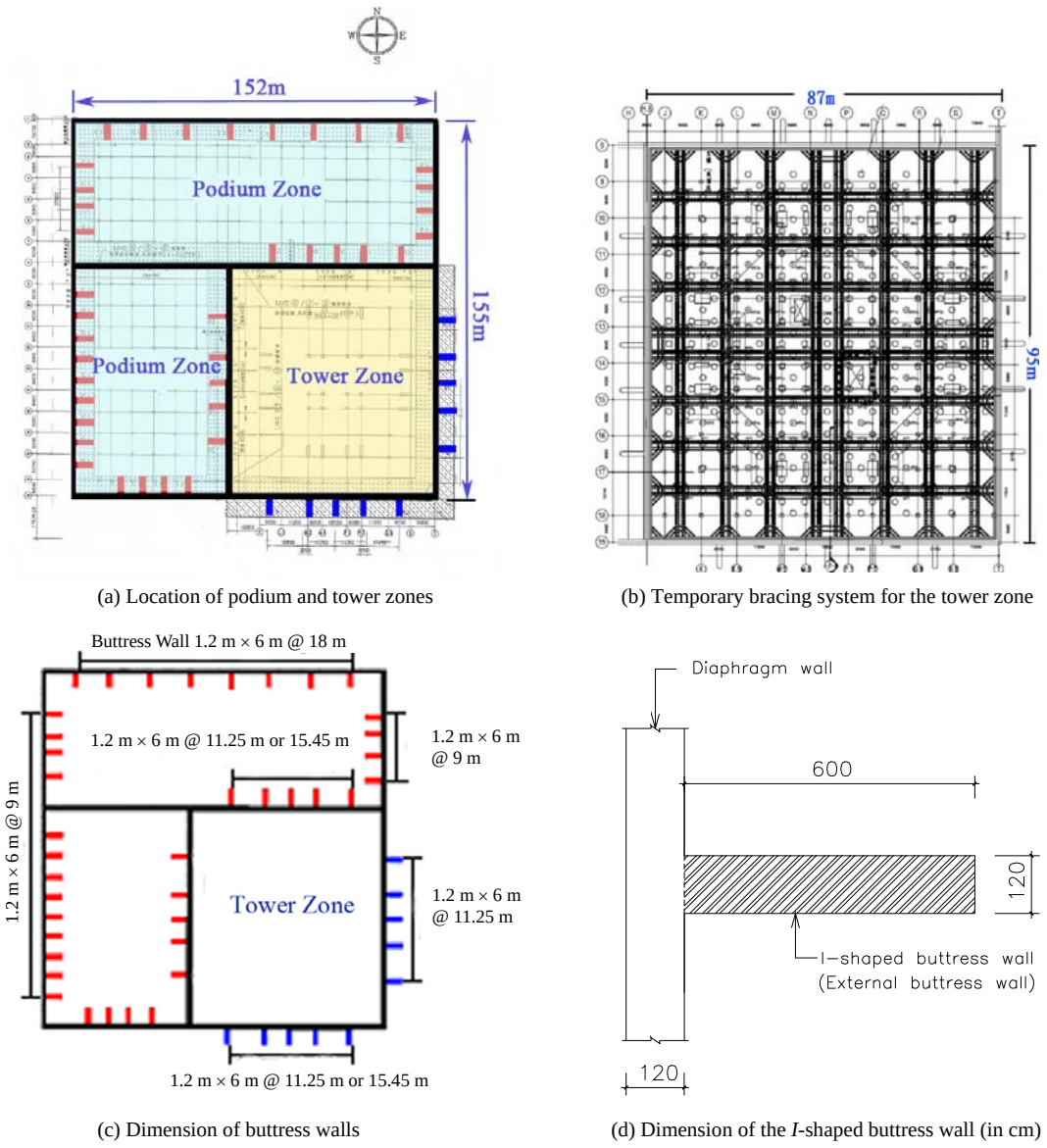

(a) Location of podium and tower zones

(b) Temporary bracing system for the tower zone

(c) Dimension of buttress walls

(d) Dimension of the *I*-shaped buttress wall (in cm)

Fig. 1 Layout of the Taipei 101project

Table 1 Effective stresses soil parameters for Taipei 101 project

Soil Layer	Depth (m)	SPT-N value	Soil Model	γ_{wet} (kN/m^3)	k_x & k_y (cm/sec)	c' (kPa)	ϕ' (°)	Ψ (°)	E' (kPa)	ν'
SF	0 ~ 2.2	12	Mohr Coulomb	17.16	1.16E-5	2	30	0	10000	0.30
CL	2.2 ~ 31	2 ~ 5	Mohr Coulomb	17.65	1.80E-7	5	26	0	26094	0.33
CL	31 ~ 39.3	22	Mohr Coulomb	17.65	0.58E-7	10	30	0	39141	0.33
SM	39.3 ~ 45.5	29	Mohr Coulomb	19.12	2.56E-5	5	34	1	58000	0.3
CL	45.5 ~ 48.9	21	Mohr Coulomb	18.63	0.90E-7	10	30	0	71700	0.33
SS	48.9 ~ 60	≥ 100	Linear Elastic	21.50	4.57E-5	–	–	–	250000	0.25

Note: γ_{wet}: wet unit weight; k_x & k_y: coefficient of permeability in *x*- and y-directions; c': cohesion; ϕ': angle of shearing resistance; Ψ: angle of dilation; E': Young's modulus; and ν': Poisson's ratio. SF: surface fill; CL: silty clay; SM: silty sand; SS: sandstone

Table 2 Parameters for diaphragm wall, concrete slab, steel struts, and buttress walls

Structural properties	Diaphragm wall	Concrete slab	Steel struts	Buttress walls
Thickness (m)	1.2	0.15 (floor slab) 3.00 (mat slab)	4H350 × 12 × 19 (1st level) 4H400 × 13 × 21 (2nd ~ 6th levels)	*I*-shaped 6 × 1.2
Material strength (MPa)	20.6	20.6	245.18	13.7
Unit weight (kN/m^3)	23.5	23.5	77.1	23.5
Young's modulus (MPa)	2.13×10^4	2.13×10^4	2.06×10^5	1.74×10^4
Poisson's ratio	0.15	0.15	0.30	0.15

Table 3 Numerical excavation procedures adopted in the Taipei 101 project

Stages	Activities
1	Construction the diaphragm and buttress walls by the "wished-in-place" method (Lin and Woo 2007).
2	Excavate the tower zone to GL.–4.4 m; Install the first level of struts (4 × H350 × 12 × 19) at GL.–3.4 m; Pre-load the struts to 320 kN.
3	Excavate the tower zone to GL.–8.4 m; Install the second level of struts (4 × H400 × 13 × 21) at GL.–7.0 m; Pre-load the struts to 400 kN.
4	Excavate the tower zone to GL.–11.3 m; Install the third level of struts (4 × H400 × 13 × 21) at GL.–10.3 m; Pre-load the struts to 480 kN.
5	Excavate the tower zone to GL.–14.3 m; Install the fourth level of struts (4 × H400 × 13 × 21) at GL.–13.3 m; Pre-load the struts to 560 kN.
6	Excavate the tower zone to GL.–16.3 m; Install the fifth level of struts (4 × H400 × 13 × 21) at GL.–15.5 m; Pre-load the struts to 560 kN.
7	Excavate the tower zone to GL.–18.9 m; Install the sixth level of struts (4 × H400 × 13 × 21) at GL.–17.7 m; Pre-load the struts to 560 kN.
8	Excavate the tower zone to the final depth at GL.–21.7 m.

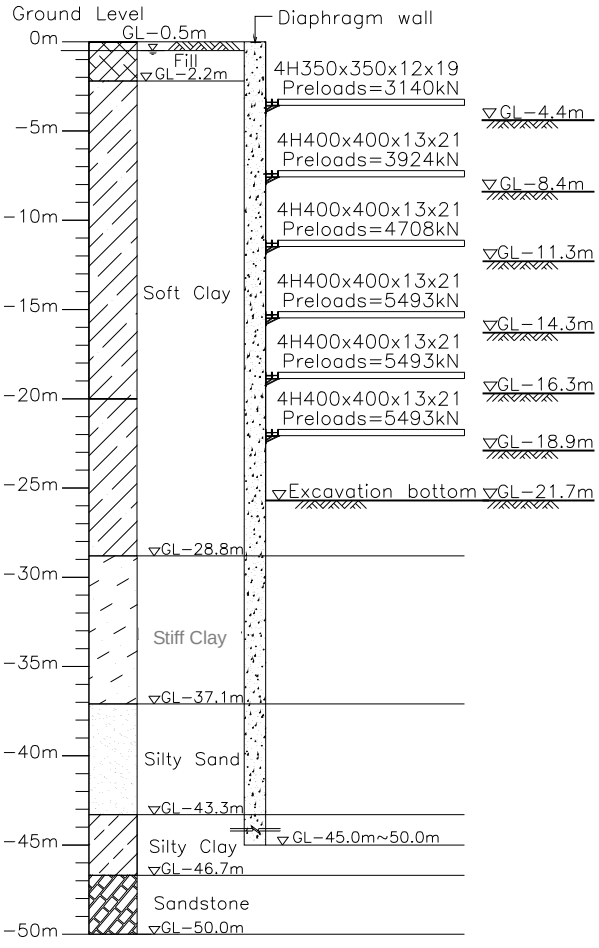

Fig. 2 Construction stages and soil stratification of the tower zone of Taipei 101

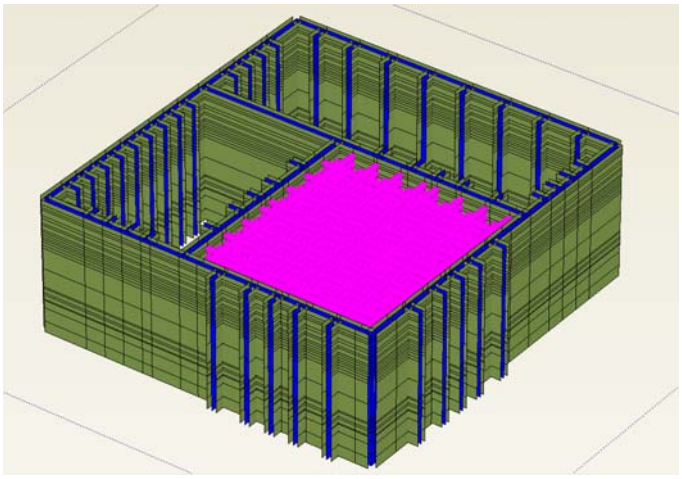

Fig. 3 A portion of the 3D numerical mesh used for Taipei 101 basement excavation

2.4 Comparison of Simulated Result and Field Data

This study aims at calibrating the three-dimensional numerical procedure of basement excavation supported by buttressed diaphragm wall. The procedure is validated through the good comparison of the simulated and field responses of the diaphragm-wall at the Tower zone. Two inclinometers, SI-3 and SI-4, had been installed in the south (Fig. 4) and east (Fig. 5) walls of the Tower zone, respectively. The simulated displacement, at locations corresponded to the location of the inclinometers SI-3 and SI-4, was thus compared to these field inclinometers data. Figures 4 and 5, respectively, compares the simulated wall displacement profile with the field inclinometers SI-3 and SI-4 during each of the excavation stages. In addition, the upper

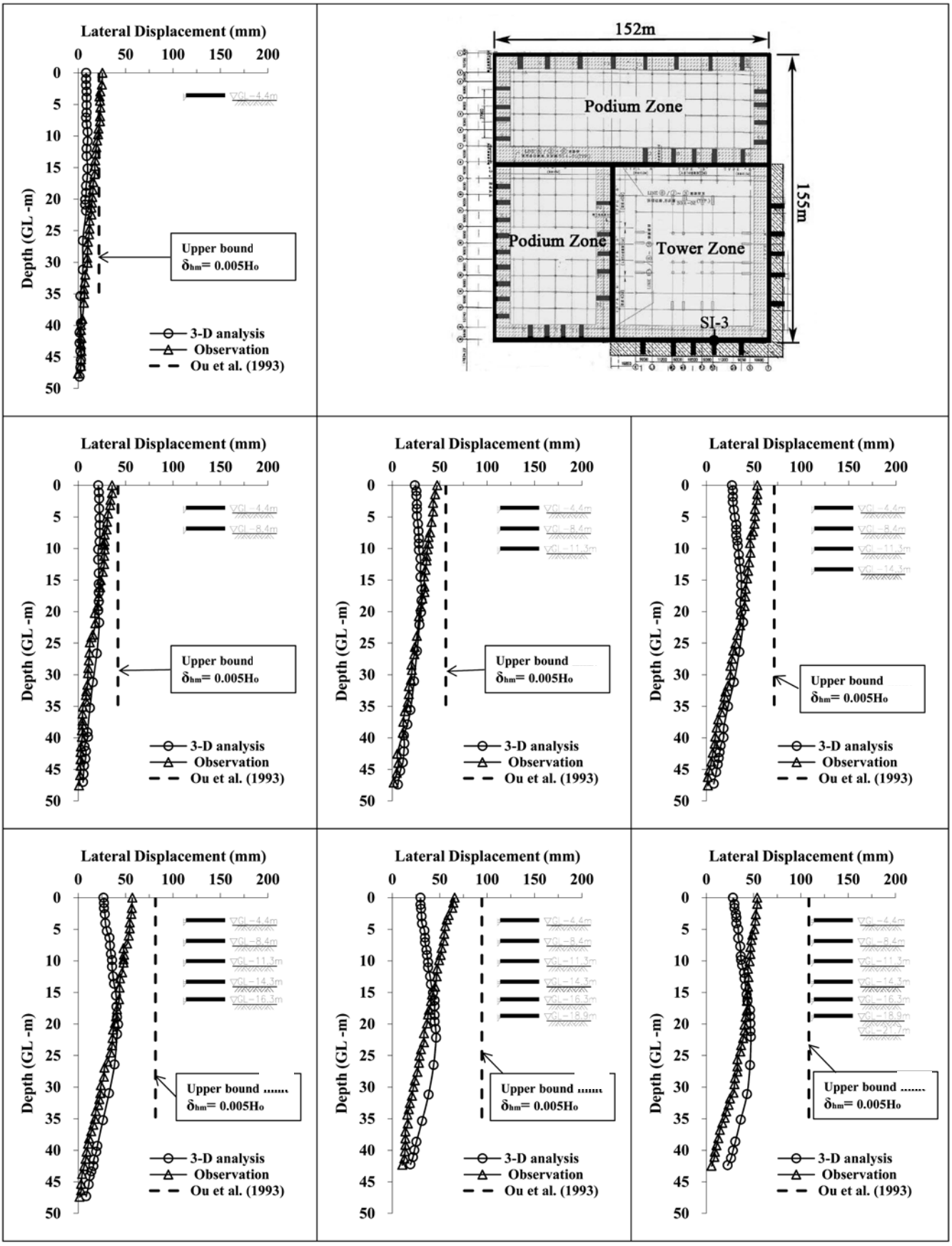

Fig. 4 Wall deformation comparisons between observed data of SI3 and numerical results at Tower Zone in Taipei 101

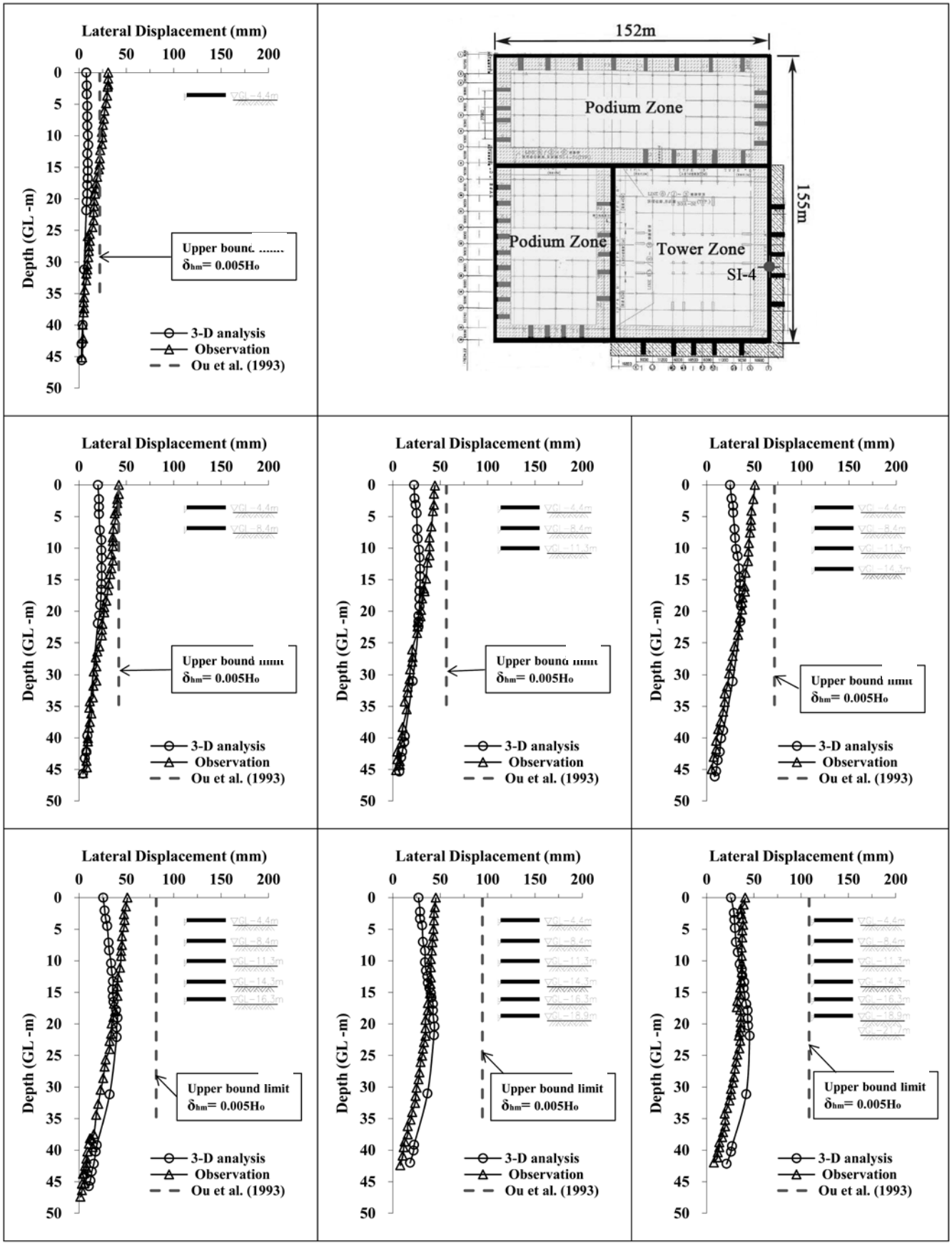

Fig. 5 Wall deformation comparisons between observed data of SI4 and numerical results at Tower Zone in Taipei 101

bound of the wall displacement estimated using the empirical equation proposed by Ou *et al*. (1993) for each of the excavation stages was also shown in these figures. As shown in Fig. 4, in general, the field displacements above the excavation level were larger than the simulated result for all the construction stages. The smaller than observed wall displacement profile obtained in the numerical analysis was perhaps due to the omission of the surcharge loading contributed by the machinery and the nearby traffics. The simulated and observed wall displacement profiles were identical below the excavation level until the excavation reached GL–16.3 m, thereafter, the simulated wall displacement profiles were seen larger than the observed profiles. Perhaps, the simulated result could be improved had a strain dependent Young's modulus been use. Figure 5 shows the comparison of the simulated and the field inclinometer SI-4 displacement profiles during each of the excavation stages. In general, the trend of the simulated results was similar to those observed in Fig. 4. Hence, the three-dimensional simulation procedure of the excavation supported by buttressed diaphragm wall could be deemed acceptable.

3. NEIHU PROJECT AND NUMERICAL ANALYSIS

3.1 Project Background and Soil Parameters

The Neihu Project is located in the Neihu District of Taipei. The project involved the excavation of an area of 44 m × 42m in plan and 9.31 m deep basement, as shown in Figs. 6 and 7, respectively. The excavation was supported by a 0.6 m thick and 21 m deep diaphragm wall. The method of construction was the bottom-up method with four excavation stages and three levels of bracing strut. The first level of bracing was strutted by the H300 × 300 × 10 × 15 structural steel members; while the second and the third levels were strutted by the H400 × 400 × 13 × 21 structural steel members (Fig. 7). Because the site was adjacent to a gas station, the safety of the gas station, and the buried oil tanks and pipelines was utmost important, especially during the excavation of the site. Hence, three *T*-shape buttress walls had been designed to provide extra stiffness to the diaphragm wall (Figs. 6a and 6b) and to minimize the wall displacement induced by the excavation. The dimension of the *T*-shaped buttress walls is shown in Fig. 6(c).

The soil parameters and the soil model used are summarized in Table 4. The Young's modulus of the silty-clay was estimated from the equation $E = 600s_u$, where the undrained shear strength s_u was taken to be 0.25 times the effective vertical stress (Ou *et al*. 2008). The Young's modulus of the silty-sand was estimated from the equation $E = 1700N$, where N is the average SPT 'N' value.

The values of the compressive strength, f_c', for the diaphragm wall and buttress walls between GL–2.0 m and GL–9.0 m were 24.5 MPa and 2 MPa, respectively. As the buttress walls between GL–9.0 m and GL–22.0 m were to be remained in place after reaching the final excavation level of 9.31 m, it has a slightly higher compressive strength of 14 MPa than the to be chipped-off buttress walls between GL–2.0 and –9.0 m. The steel struts have the same Young's modulus as those used in the Taipei 101 project. Again, a reduction factor of 0.6 has to be applied to the above values to cater for the concrete cracking due to wall deformation and the possibility of poor construction quality.

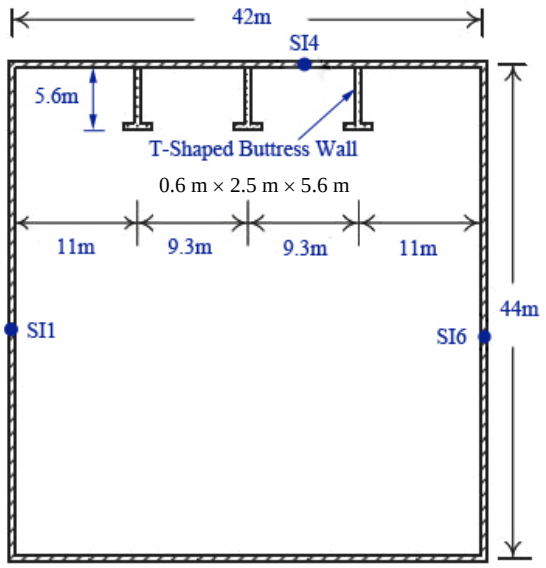

(a)

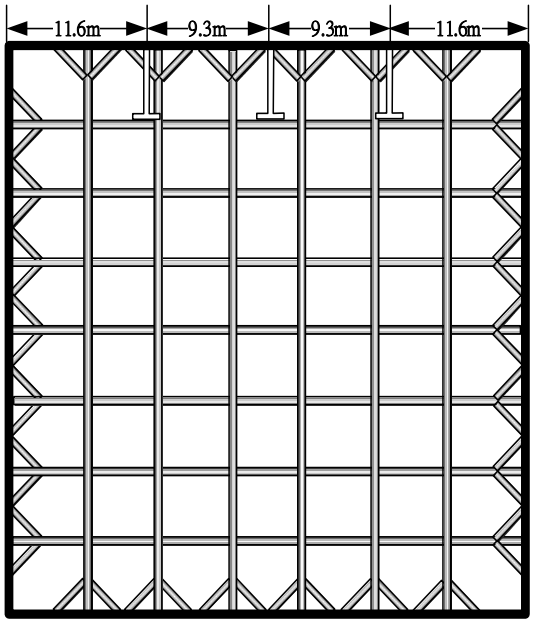

(b)

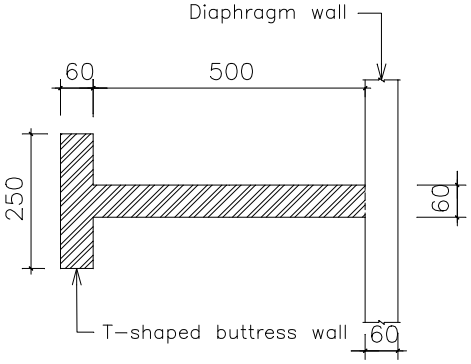

(c)

Fig. 6 (a) Layout of the excavation site; (b) temporary bracing system; and (c) dimension (in cm) of *T*-shaped buttress walls adopted in Neihu project (after Wang 1998)

Table 4 Effective stress soil parameters for Neihu project (after Wang 1998)

Soil Layer	Depth (m)	SPT-N	Model	γ_{wet} (kN/m^3)	k_x & k_y (cm/sec)	c' (kPa)	ϕ' (°)	Ψ (°)	E' (kPa)	ν'
CL	0 ~ 20	1 ~ 4	Mohr Coulomb	17.64	1.25E-7	0.1	24	0	10570	0.35
SM	20 ~ 26	7 ~ 36	Mohr Coulomb	19.60	3.25E-4	0.1	30	0	37000	0.30

Note: γ_{wet}: wet unit weight; k_x & k_y: coefficient of permeability in *x*- and *y*-directions; c': cohesion; ϕ': angle of shearing resistance; Ψ: angle of dilation; E': elastic modulus; and ν': Poisson's ratio. CL: silty clay; SM: silty sand

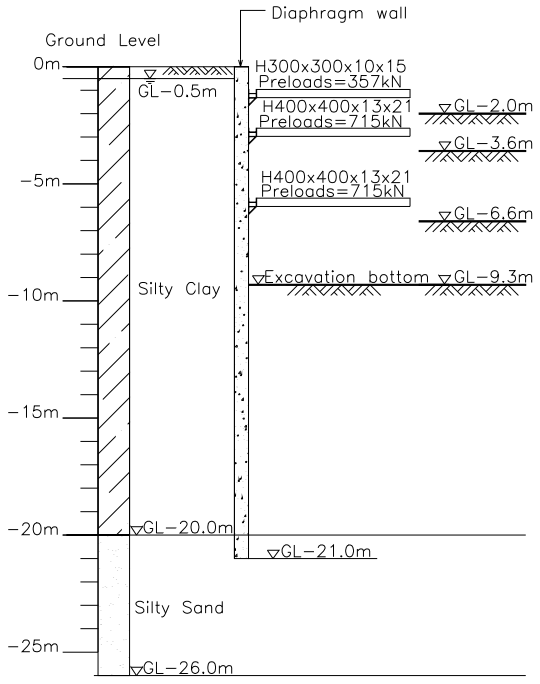

Fig. 7 Construction stages and soil stratification of the Neihu project

Table 5 Numerical excavation procedures adopted in the Neihu project

Stages	Activities
1	Excavate to 2 m below the ground level; Install the first level of struts at GL−1.15 m; Pre-load the struts to 350 kN.
2	Excavate to GL−.36 m; Install the second level of struts at GL−2.8 m; Pre-load the struts to 710 kN.
3	Excavate to GL.−6.6 m; Install the third level of struts at GL−5.8 m; Pre-load the struts to 710 kN.
4	Excavate to the final depth of 9.31 m.

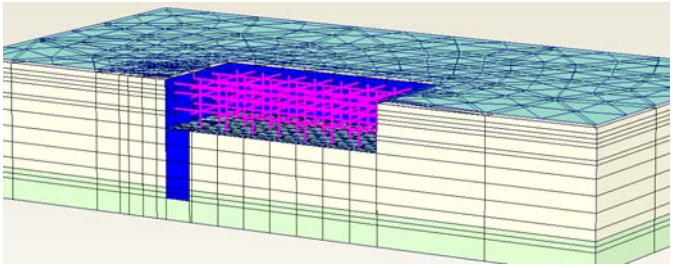

Fig. 8 3D finite element mesh used in the analysis

3.2 Numerical Modeling

A three-dimensional analysis has been conducted for the Neihu Project. Only half of the site was modeled, *i.e.* symmetric with respect to the center lines of the width. The boundary of the numerical model was set at 5 times the excavation depth from each side of the diaphragm wall with the assumption that no displacement would be generated in the soil beyond the distance of 5 times the excavation depth. The three-dimensional finite element mesh used is shown in Fig. 8 while the numerical excavation procedure for this analysis is shown in Table 5.

3.3 Comparison of Simulated Result and Field Data

Figures 9 and 10, respectively, shows the wall displacement profile recorded by the inclinometers SI-4 and SI-6 during each of the four excavation stages. It can be seen that the recorded displacement of the diaphragm wall with the *T*-shape buttress walls (Fig. 9) was significantly lower than that of the wall without the buttress walls (Fig. 10), in particular, during the third and fourth stages of the excavation. The simulated displacement is compared to the field inclinometers SI-4 and SI-6 data in Figs. 9 and 10, respectively. Figure 9 shows that the simulated displacement profile of the diaphragm wall was similar to that recorded by the inclinometer SI-4, which was installed between two *T*-shaped buttress walls, albeit, the simulated results were larger than the field recorded data. The over-estimation of the simulated displacement was probably due to the use of a less stiff silty-clay in the Neihu project compared to the stiffer silty-clay in the Taipei 101 project.

As for the east wall, which was without buttress walls, the simulated wall displacement profile was rather similar in shape to that recorded by the inclinometer SI-6 during the first and, perhaps, the second： stages of excavation (Fig. 10), albeit the simulated results over-estimated the field data as in the case of the diaphragm wall with buttress walls. For the third and fourth levels of the excavation, both the simulated and field displacement profiles have the same deep inward shape. However, the numerical analysis over-estimated the wall displacement for depth between GL 0 to −5 m but under-estimated the wall displacement

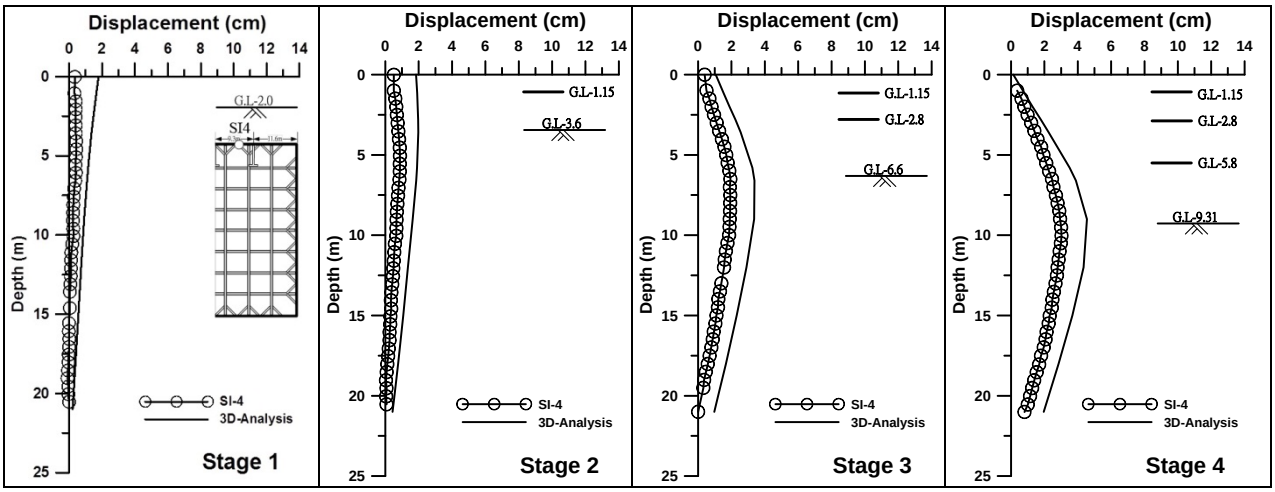

Fig. 9 Comparison of simulated and SI-4 field displacement results (diaphragm wall with buttress walls)

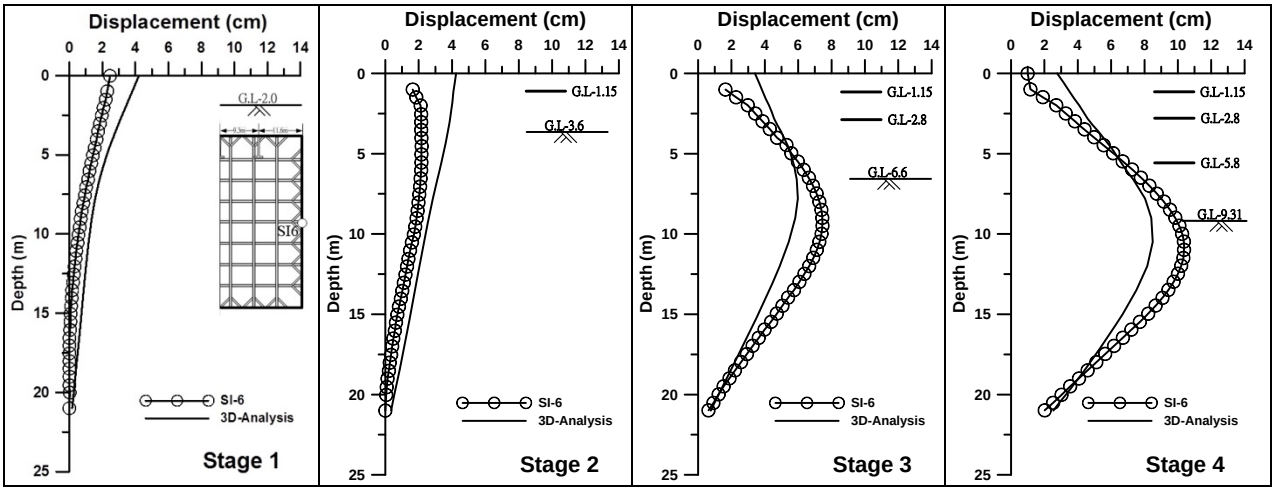

Fig. 10 Comparison of simulated and SI-6 field displacement results (diaphragm wall without buttress walls)

for depth greater than GL−5 m. This phenomenon can also be seen in Fig. 6 of Ou *et al*. (2008), who also calibrated their three-dimensional numerical procedure against the Neihu project. However, no explanation was given in Ou *et al*. (2008); instead they have concluded that "the computed wall deflections were, in general, in close agreement with the observed wall deflections." The results in Figs. 9 and 10 showed that three-dimensional simulation is, in general, effective in modeling the response (displacement profile) of diaphragm wall with buttress walls during deep excavation. To obtain a perfect match in terms of the magnitude of the displacement, a more sophisticated soil model and simulation procedure must first be derived.

4. EFFICIENCY STUDY FOR VARIOUS TYPES OF BUTTRESS WALLS

The consistent pattern of the result between the simulated and field observed wall displacement profiles for the above two projects revealed that three-dimensional modeling is suitable and reliable in the simulation of supported excavation with buttressed diaphragm wall. Because the excavation geometry of the Neihu project is less complicated than the Taipei 101 project, the Neihu project has been chosen here as the model for use in the study of the efficiency of buttress wall. As seen in Figs. 9 and 10, the displacement of the wall with buttresses is significantly less than that of the wall without buttresses. The ratio of the displacement reduced by buttressed diaphragm wall to the energy supplied for its operation. Thus, one may define the efficiency of the buttress walls as a displacement reduction ratio, DRR, through

$$\mathrm{DRR} = \frac{\delta_{hm} - \delta_{hmb}}{\delta_{hm}} \tag{1}$$

where δ_{hm} is the maximum horizontal displacement of the diaphragm wall without buttress walls, and δ_{hmb} is the maximum horizontal displacement of the diaphragm wall with buttress walls. The maximum displacement of the diaphragm wall without buttress walls, δ_{hm}, is a constant in Eq. (1). Hence, an increase in the value of the DRR means that a smaller maximum displacement has been observed for the buttressed diaphragm wall. Thus, the higher the value of the DRR the more efficient that buttressed diaphragm wall is. Using this ratio, the influences of the shape (rectangular, called the *I*-shaped buttress wall here, and *T*-shaped buttress wall), and the thickness of the buttress wall are examined here. The configurations of the *I*-shaped and *T*-shaped have been shown in Figs. 11 and 6(c), respectively.

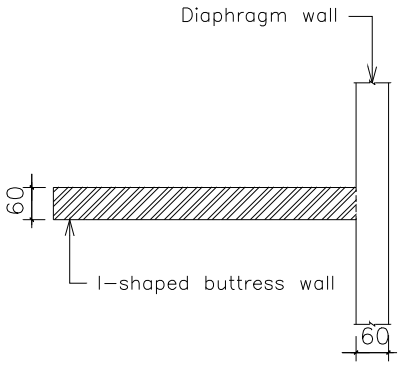

Fig. 11 Details of *I*-shaped buttress wall (unit in cm)

4.1 Influence of Shape and Normalized Thickness of Buttress Walls

Figure 12(a) shows the relationship between the DRR and the normalized buttress wall thickness, t_{BW} / t_W (*i.e.* the ratio of the buttress wall thickness, $t_{BW,}$ to the diaphragm wall thickness, t_W). Four cases have been considered here: (A) use of the internal *I*-shaped buttress walls with walls chipped-off during each excavation stage, (B) use of the internal *T*-shaped buttress walls with walls chipped-off during each excavation stage, (C) use of the internal *T*-shaped buttress walls with walls not chipped-off during each excavation stage, and (D) use of the external *T*-shaped buttress walls and they were not chipped-off during each excavation stage. The locations of the *I*- or *T*-shaped buttress walls in Cases A, B and C were identical to that shown in Fig. 6(a). As for Case D, the external buttress walls were located outside the diaphragm wall and opposite to that shown in Fig. 6(a). For the range of the study normalized thickness (0.67 ~ 2.0), the range of the DRR of Case A was 21 ~ 26%, for Case B was 33 ~ 38%, for Case C was 46 ~ 49%, and for Case D was 35 ~ 46%. This indicates that the *I*-shaped buttress wall with 21% < DRR < 26% in Case A was less efficient than the *T*-shaped buttress wall with 33% < DRR < 38% in Case B. The *T*-shaped buttress wall would be even more efficient in restraining the diaphragm wall displacement had the internal *T*-shaped buttress wall was not chipped-off during each excavation stage (Case C with 46 < DRR < 49%).

The effect of the thickness of the buttress walls on the maximum displacement of the diaphragm wall can also be observed in Fig. 12(a). In all cases, the thickness of the diaphragm wall, t_W, used was 0.6 m while the thicknesses of the buttress walls, t_{BW}, used were 0.4 m, 0.6 m, 0.8 m, 1.0 m and 1.2 m. The t_{BW} / t_W ratio increases as the thickness of the buttress wall increases. Hence, cases A and B in Fig. 12(a) indicate that increasing the thickness of the buttress wall from t_{BW} / t_W = 0.67 to t_{BW} / t_W = 2.0 would not always result in the efficient use of the buttress wall. If the buttress wall was to be chipped-off during each excavation stage, the DRR remains reasonably the same or decreased slightly with the increase of the t_{BW} / t_W ratio. This was because the maximum diaphragm wall displacement always occurred above or around the excavation level at which the buttress walls had been chipped-off concurrently with the excavation. Thus, increasing the thickness of the buttress walls from t_{BW} / t_W = 0.67 to t_{BW} / t_W = 2.0 would not serve any purpose in reducing the maximum displacement of the diaphragm wall. However, if either the *T*-shaped internal (Case C) or external

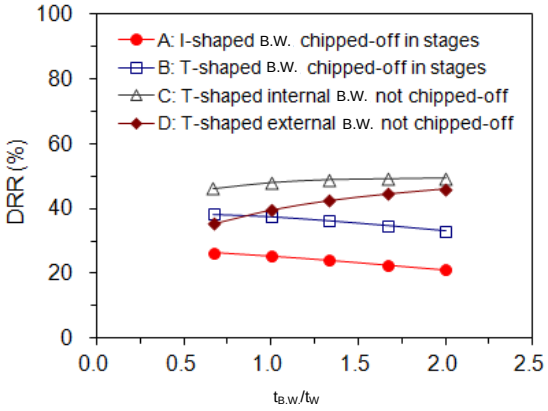

(a)

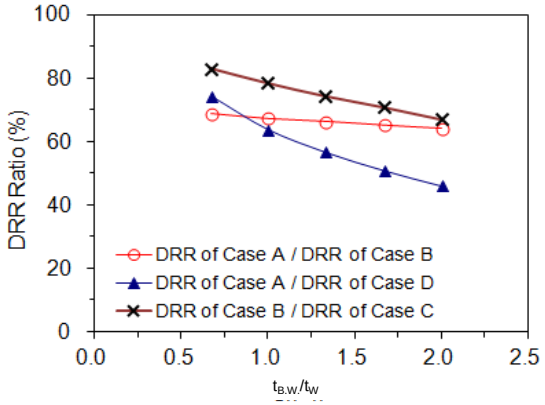

(b)

Fig. 12 Relationship of (a) DRR, and (b) DRR ratio with respect to normalized buttress wall thicknesses

(Case D) buttress walls, which were not chipped-off throughout the excavation, were used, the DRR now increases with the increase of the t_{BW} / t_W ratio. This indicated that the increase of the thickness of the buttress walls was only effective in restraining the maximum displacement of the diaphragm wall in the case where the buttress walls were not chipped-off during excavation stages.

Figure 12(b) shows the relationship between the ratios of the DRR of the *I*-shaped internal buttress walls to the DRR of the *T*-shaped internal buttress walls and the normalized thicknesses. The DRR ratio of Case A over Case B ranged between 64% ~ 68%, which was almost constant for the range of the normalized buttress wall thickness studied. Thus, the efficiency of the *I*-shaped internal buttress walls was about 64 ~ 68% of that of the *T*-shaped internal buttress walls for 0.67 ≤ t_{BW} / t_W ≤ 2.0. As for the cases of the *I*-shaped internal buttress walls (case A) and the *T*-shaped external buttress walls (case D), the ratio decreased from 74% for t_{BW} / t_W = 0.67 to 46% for t_{BW} / t_W = 2.0. This indicated that the efficiency of the *I*-shaped internal buttress walls was about 74% of that of the *T*-shaped external buttress walls for t_{BW} / t_W = 0.67; however, if the normalized thickness of the buttress walls increases to 2.0 the efficiency of the *I*-shaped internal buttress walls decreased to just 46%. Thus, the external buttress walls were more efficient in restraining the maximum displacement of the diaphragm wall. The DRR ratio of case B (*T*-shaped

buttress walls, chipped-off each stage) to case C (*T*-shaped buttress walls not chipped-off) was 83% ~ 67% for $0.67 \leq t_{BW} / t_W \leq 2.0$. This result simply confirmed that the buttress walls not chipping-off during excavation were more efficient than the chipped-off buttress walls.

4.2 Influences of Length and Spacing of External Buttress Walls

To examine the influences of length and spacing of the external buttress walls on diaphragm wall displacement, a model with an excavation area of 72 m × 60 m in plan has been created for analysis. The soil parameters, concrete strength and penetration depth of both the external buttress walls and diaphragm wall, and the number of excavation stages and support system were all identical to that used in the Neihu project. To avoid complication, pre-load was not applied to the struts as in the case of the Neihu project. The influence of the spacing of the external buttress walls has been studied by varying the buttress walls spacing between 6, 9, 12, 18, and 36 m; and for each of the above spacing, the influence of the length of the external buttress walls has also been studied by varying the length of the buttress wall between 2, 5, 8, 10, and 15 m. To reduce the computing time, only a quarter of the area was modeled in the analysis.

Figure 13(a) shows the lateral displacement of the diaphragm wall either without or with an external buttress wall located 36 m from the corner. It can be seen that, for the case without the external buttress wall, the maximum lateral displacement was about 8.4 cm. The corner effect was found to cover a distance of about 18 m, which was about two times the excavation depth (= 9.31 m), from the corner of the diaphragm wall. The distance of the corner effect was almost similar for all the buttresses lengths studied. In general, the lateral displacement at the middle section of the diaphragm wall was inversely proportional to the length of the buttresses. Figures 13(b) and 13(c) show the diaphragm wall displacement where the spacing of the external buttress walls was 18 m and 12 m, respectively. Clearly, the lateral displacement of the diaphragm wall decreases, in particular, at the location where the buttress walls were located. Figures 13(d) and 13(e) show the diaphragm wall displacement where the spacing of the external buttress walls was 9 m and 6 m, respectively. The lateral displacement profile of the diaphragm wall was almost similar in both cases, albeit the 9 m-spacing profile was not as smooth as the 6 m-spacing profile. Thus, the optimum spacing of the external buttress walls was about two times the excavation depth.

Figure 13(f) shows the relationship between the DRR and the ratio of the spacing of the buttress wall, S_{BW}, to the excavation depth, H_e, for various lengths of buttress wall, LB. From the definition of the DRR, as given in Eq. (1), the maximum horizontal displacement of the diaphragm wall for various buttress walls spacing and lengths have been obtained and used to derive Fig. 13(f). For a particular length of the buttress walls, the DRR decreases exponentially to S_{BW} / H_e of about 2; thereafter, the DRR remains almost constant. This means that as the spacing of the buttress walls increases, the maximum lateral displacement of the diaphragm wall becomes larger, and hence the efficiency of such buttress walls drops. For all the lengths studied, it was clear that to improve the buttress wall efficiency the spacing of the buttress walls should be selected at less than two times the excavation depth, preferably, at one excavation depth.

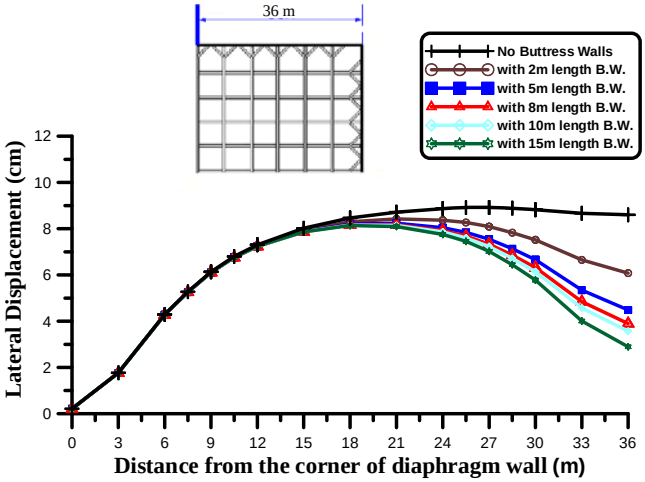

(a) Case of buttress walls spacing of 36 m

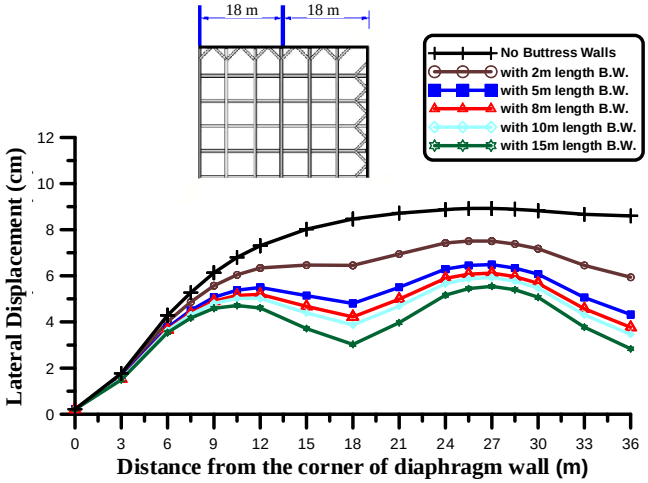

(b) Case of buttress walls spacing of 18 m

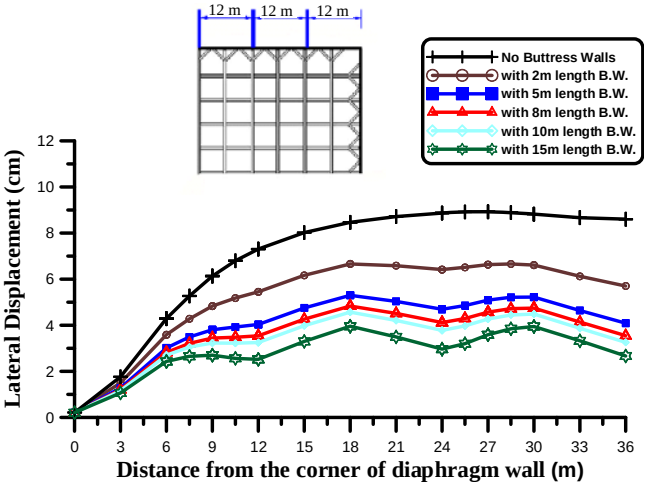

(c) Case of buttress walls spacing of 12 m

Fig. 13 (a) ~ (e) Influence of spacing and length of buttress walls on diaphragm wall displacement; and (f) relationship of displacement reduction ratio (DRR) and normalized spacing of external buttress walls

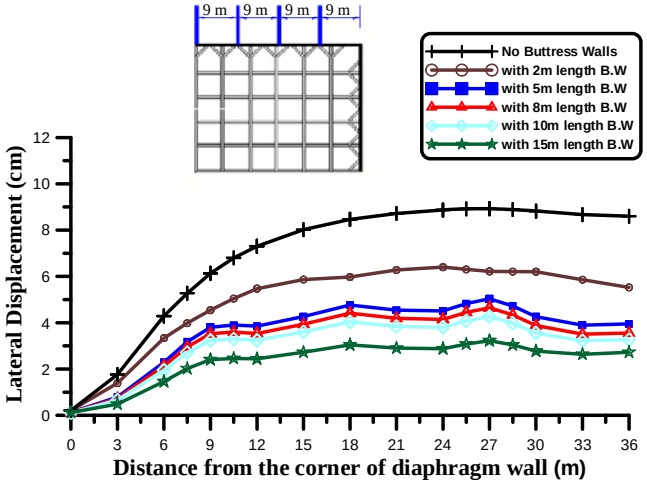

(d) Case of buttress walls spacing of 9 m

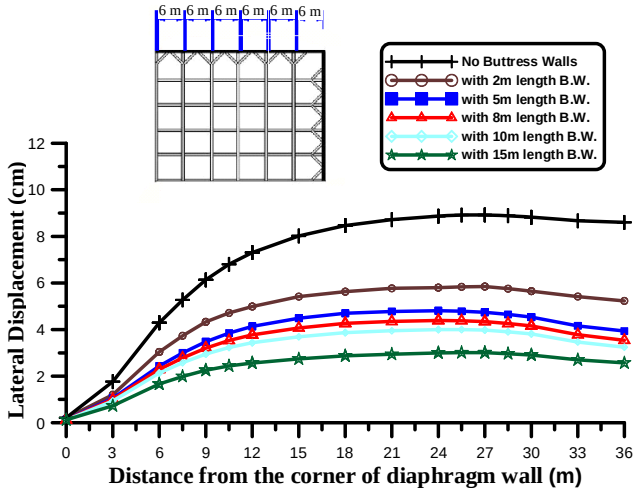

(e) Case of buttress walls spacing of 6 m

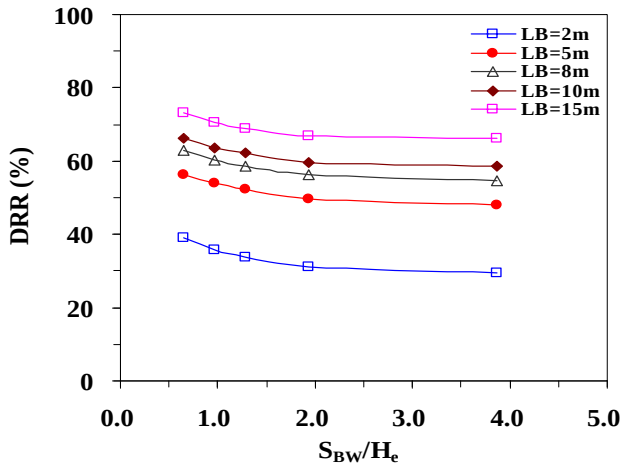

(f) Normalized spacing of external buttress walls versus DRR

Fig. 13 (continued)

5. CONCLUSIONS

Based on the results of a series of parametric study, which had been calibrated against the field data of the Taipei 101 and Neihu basements excavation projects, the following conclusions can be made:

1. From the results of the displacement reduction ratio, DRR, versus normalized buttress wall thickness, it can be concluded from the four buttress walls layout studied that the most efficient buttress walls layout was the internal buttress walls that were not sequentially removed until the final excavation level was reached. However, from the practical point of view (because the internal buttress walls could obstruct the basement construction work and would be cumbersome to chip-off without further providing properly propped scaffoldings), the most efficiency layout should be the external buttress walls where there is no need to remove the buttress walls at all even after the completion of the excavation work. It is recommended that the external buttress walls should be considered for deep excavation project.
2. It was found that the internal *T*-shaped buttress walls were more efficient than the internal *I*-shaped buttress walls on reducing the displacement of the diaphragm wall.
3. For the range of the study ($6 \le S_{BW} \le 36$ m with excavation depth, H_e, of 9.31 m), the displacement of the diaphragm wall was decreasing non-linearly with the increase of the normalized spacing, S_{BW} / H_e of the buttress walls of length ranges between 2 to 15 m. The result implied that the effective spacing of the buttress walls should not be more than two times the excavation depth.

REFERENCES

Brinkgreve, R. B. J. and Swolfs, W. M. (2007), *PLAXIS 3D Foundation: Material Models Manual Version 2*. Plaxis bv, Delft, The Netherlands.

Finno, R. J., Blackburn, J. T., and Roboski, J. F. (2007), "Three-dimensional effects for supported excavations in clay." *Journal of Geotechnical and Geoenvironmental Engineering*, ASCE, **133**(1), 30-36.

Hsieh, H. S. and Lu, F. G. (1999), "A note of the analysis and design of diaphragm wall with buttresses." *Sino-Geotechnicals*, **76**, 39-50.

Lin, D. G. and Woo, S. M. (2005), "Geotechnical analyses of Taipei International Financial Center (Taipei 101) construction project." *Proc. of 16th Int. Conf. on Soil Mechanics and Geotechnical Engineering*, Osaka, Japan, 1513-1516.

Lin, D. G. and Woo, S. M. (2007), "Three dimensional analyses of deep excavation in Taipei 101 construction project." *Journal of GeoEngineering*, TGS, **2**(1), 29-41.

Ou, C. Y., Chiou, D. C., and Wu, T. S. (1996), "Three-dimensional finite element analysis of deep excavations." *Journal of Geotechnical Engineering*, ASCE, **122**(5), 337-345.

Ou, C. Y., Hsieh, P. G., and Chiou, D. C. (1993), "Characteristics of ground surface settlement during excavation." *Canadian Geotechnical Journal*, **30**, 758-767.

Ou, C. Y., Liao, J. T., and Lin, H. D. (1998), "Performance of a top-down basement construction." *Journal of Geotechnical and Geoenvironmental Engineering*, ASCE, **124**(9), 798-808.

Ou, C. Y., Teng, F. C., Seed, R. B., and Wang, I. W. (2008), "Using buttress walls to reduce excavation-induced movements." *Geotechnical Engineering*, ICE, **161**(4), 209-222.

Wang, Y. W. (1998), *A Study of Measures for Reducing Wall Deflection in Deep Excavation*. Master Thesis, National Taiwan University of Science and Technology, Taiwan.

Yu, C. H. (2011), "On design and construction of pile group foundation of Taipei 101." *Geotechnical Engineering Journal*, SEAGS & AGSSEA, **42**(2), 56-69.